

**Rapid conversion of *Pseudomonas aeruginosa* to a spherical cell morphotype facilitates tolerance to carbapenems and penicillins but increases susceptibility to antimicrobial peptides**

Leigh G. Monahan<sup>1</sup>, Lynne Turnbull<sup>1</sup>, Sarah R. Osvath<sup>1</sup>, Debra Birch<sup>2</sup>, Ian G. Charles<sup>1</sup>, and  
Cynthia B. Whitchurch<sup>1#</sup>

<sup>1</sup>The itthree institute, University of Technology Sydney, Ultimo, NSW, Australia

<sup>2</sup>Microscopy Unit, Faculty of Science, Macquarie University, North Ryde, NSW, Australia

**# Correspondence to:** Cynthia.Whitchurch@uts.edu.au

**Running title:**  $\beta$ -lactam tolerance enhances AMP susceptibility

## Abstract

The Gram negative human pathogen *Pseudomonas aeruginosa* is able to tolerate high concentrations of  $\beta$ -lactam antibiotics. Despite inhibiting the growth of the organism, these cell wall-targeting drugs exhibit remarkably little bactericidal activity. However, the mechanisms underlying  $\beta$ -lactam tolerance are currently unclear. Here we show that *P. aeruginosa* undergoes a rapid *en masse* transition from normal rod shaped cells to viable, cell wall defective spherical cells when treated with  $\beta$ -lactams from the widely used carbapenem and penicillin classes. When the antibiotic is removed, the entire population of spherical cells quickly converts back to the normal bacillary form. Our results demonstrate that these rapid population-wide cell morphotype transitions function as a strategy to survive antibiotic exposure. Taking advantage of these findings, we have developed a novel approach to efficiently kill *P. aeruginosa* by using carbapenem treatment to induce *en masse* transition to the spherical cell morphotype and then exploiting the relative fragility and sensitivity of these cells to killing by antimicrobial peptides (AMPs) that are relatively inactive against *P. aeruginosa* bacillary cells. This approach could broaden the repertoire of antimicrobial compounds used to treat *P. aeruginosa* and serve as a basis for developing new therapeutics to combat bacterial infections.

## Introduction

*Pseudomonas aeruginosa* is a major human pathogen and a leading cause of hospital-acquired infections. *P. aeruginosa* infections are difficult to eradicate and are often fatal, which is in part due to the organism's high intrinsic resistance to a variety of different antimicrobials (1). The mechanisms underlying intrinsic antibiotic resistance in *P. aeruginosa* are largely well understood. However, an important and as yet unexplained observation is the ability of *P. aeruginosa* to survive in the presence of high concentrations of the cell wall-targeting  $\beta$ -lactam antibiotics.

$\beta$ -lactams are a broad class of antibiotics that include penicillin derivatives, cephalosporins, monobactams, and carbapenems. They are the most widely used group of antibiotics in the world (2) and mediate bacterial killing primarily by inhibiting the enzymes, known as penicillin-binding proteins or PBPs, that catalyse the formation of peptidoglycan cross-links in the bacterial cell wall (3).  $\beta$ -lactams drugs typically exhibit bactericidal activity against susceptible organisms (4), and this is often associated with changes in bacterial morphology and the formation of spherical or filamentous cells that are prone to lysis (3, 5-8).

Interestingly, despite inhibiting cell growth,  $\beta$ -lactams have been found to have very little bactericidal activity against *P. aeruginosa* (9-13). This intrinsic tolerance of  $\beta$ -lactams likely accounts for the fact that when treating *P. aeruginosa* infections, optimal microbiological outcomes occur when  $\beta$ -lactam concentrations are maintained at 4-6.6 x the minimal inhibitory concentration (MIC) throughout the majority of the dosing period (13). Furthermore,  $\beta$ -lactam tolerance by *P. aeruginosa* can lead to the emergence of spontaneous  $\beta$ -lactam resistant strains

(12, 14). Thus  $\beta$ -lactam tolerance provides significant challenges for clinicians when treating *P. aeruginosa* infections. The mechanisms underlying this tolerance, however, are unclear.

Here we show that tolerance of *P. aeruginosa* to several  $\beta$ -lactams, including carbapenems and a penicillin derivative, is mediated by a rapid population-wide transition to a viable, cell wall defective spherical form. We demonstrate that these spherical cells can survive in the presence of antibiotic and quickly revert to the normal bacillary mode of growth following its removal. Our results indicate that transition to the spherical cell morphotype likely does not require the acquisition of specific mutations but rather is an intrinsic response to antibiotic exposure that serves as a survival strategy. Significantly, we further demonstrate that *P. aeruginosa* can be efficiently killed by combining the  $\beta$ -lactam meropenem with antimicrobial peptides that show little to no activity against bacillary cells of *P. aeruginosa*. We propose that such combination treatments could provide a novel approach for antibacterial therapy.

## **Materials and Methods**

### *Bacterial strains, media and growth conditions*

*P. aeruginosa* strains used in this study were PA14, PAO1, PA103, PAK, ATCC27853, PAE27 (otitis externa isolate, Gribbles Pathology, Melbourne, Australia) and PA911 (cystic fibrosis lung isolate, Monash Medical Centre, Melbourne, Australia). All experiments were performed with strain PA14 unless otherwise indicated. Cells were grown either in cation-adjusted Mueller Hinton broth (CAMHB; Fig. 1), synthetic cystic fibrosis sputum medium (15) (Fig. S1A), fetal bovine serum (Fig. S1B) or CAMHB supplemented with 0.5 M sucrose (Fig. 2-7 and Fig. S2-S3). To induce spherical cell formation, cultures were grown to early-exponential phase at 37°C with



vigorous shaking, antibiotic was added and cells were then incubated without shaking at 37°C. For reversion, spherical cells were pelleted by centrifugation at 3,000 g for 10 min, resuspended in antibiotic-free media and grown with static incubation at 37°C. Antibiotics were used at 5x MIC, as determined against strain PA14 using standard methods (16). MIC values for PA14 were as follows: meropenem, 1 µg/mL; imipenem, 2 µg/mL; carbenicillin, 128 µg/mL. MIC values for meropenem were also determined against each strain used in the study and were found to be between 1-2 µg/mL for all strains.

### *Phase-contrast and fluorescence microscopy*

To prepare samples for phase-contrast imaging, a 1.0 X 1.0 cm square well was set up on the surface of a glass microscope slide by attaching a 25 µL Gene Frame (ABgene). The well was filled with 25 µL of culture and a coverslip was placed on top. For fluorescence microscopy (live/dead staining and super resolution 3D-SIM), 200 µL of cells were applied to a 35 mm sterile glass bottom FluoroDish (World Precision Instruments). Membrane stain FM1-43FX (5 µg/mL; Life Technologies) was added to the sample before applying to the dish for 3D-SIM. Syto9 (5 µM; Life Technologies) and propidium iodide (30 µM; BD) were added for live/dead staining.

An Olympus IX71 wide-field inverted microscope was used for phase-contrast imaging, a Zeiss Axioplan 2 fluorescence microscope was used for imaging of live/dead stained cells and a DeltaVision OMX-Blaze™ (Applied Precision Inc.) was used for 3D-SIM (17). Images were processed as described previously (17), analysed and presented using AnalySIS Research Pro (Olympus), AxioVision (Zeiss) or IMARIS (Bitplane) software.

*Transmission electron microscopy (TEM)*

To prepare samples for TEM, cells were pelleted by centrifugation at 3,000 g for 10 min and resuspended in a fixative solution of 2% glutaraldehyde in phosphate buffered saline (PBS; 0.1M, pH 7.2) containing 0.1 M sucrose. Cells were fixed overnight at 4°C, then washed three times in PBS. Cell pellets were embedded in 1% low melt agarose (J.T. Baker Inc.) and agarose blocks were cut into 1 mm cubes, transferred to glass vials and post-fixed in 1% osmium tetroxide (OsO<sub>4</sub>) in PBS for 1 h at room temperature. Following post-fixation, samples were washed in distilled water three times for 5 min each wash and immersed in 2% aqueous uranyl acetate for 30 min. Cell pellets were dehydrated through a graded series of ethanols (50-100%), infiltrated and subsequently embedded in L. R. White Resin (London White Resin Company). Ultra-thin (70 nm) sections were cut using a Reichert ultramicrotome (Ultracut S, Leica Microsystems) and mounted onto pioloform-coated, 300 mesh, thin-bar copper grids. Grids were stained with saturated aqueous uranyl acetate (7.7%) for 30 min and Reynold's lead citrate for 4 min. Samples were examined using a Philips CM0 transmission electron microscope equipped with a Megaview III TEM CCD camera and iTEM image capture software (Olympus). Digital images were processed for publication using Adobe Photoshop CS version 8.0 (Adobe Systems). All TEM materials were supplied from ProScitech, Australia.

*Viability assays*

To estimate the number of viable cells in culture, 10-fold dilutions were plated in triplicate onto LB medium containing 1.6% agar (without antibiotics) and incubated overnight at 37°C. Colonies were counted and viability was calculated as the number of colony forming units (CFUs) per mL of culture.

## Results

*P. aeruginosa* cells rapidly convert to a viable spherical morphotype when treated with meropenem

As an initial approach to understand  $\beta$ -lactam tolerance by *P. aeruginosa*, we monitored *P. aeruginosa* cells under the microscope following treatment with meropenem, a broad-spectrum carbapenem antibiotic that is commonly used to treat *P. aeruginosa* infections in humans. It has been noted in previous studies that *P. aeruginosa* cells switch to a spherical morphology when exposed to meropenem (7, 8). We hypothesized that this spherical morphotype may be a viable alternative form of the bacterium that mediates survival in the presence of the antibiotic.

To test this, *P. aeruginosa* strain PA14 was first cultured in a standard laboratory growth medium (cation-adjusted Mueller Hinton broth) and treated with a clinically relevant dose of meropenem (5x MIC). Cells were then visualized at regular intervals using conventional phase-contrast microscopy. In the presence of meropenem, we observed a rapid and efficient conversion of the entire population from normal rod shaped cells to apparently spherical cells (Fig. 1A-E). Just 1 h after the addition of the antibiotic a large proportion of cells (65%) had clearly begun transitioning to the spherical morphology. Most cells (67%) had completed the transition by 4 h, and after 24 h the entire population consisted only of spherical cells (Fig. 1E). To determine if these spherical cells were viable we co-stained PA14 with the fluorescent dyes Syto9 and propidium iodide after 24 h exposure to meropenem. This approach differentiates viable cells, which only stain with Syto9 (green), from dead cells that also stain with propidium iodide (red) (Fig. 1F, G). These assays showed that the vast majority of spherical cells in the population (84%) were viable and thus able to tolerate exposure to 5x MIC of the antibiotic.

The remaining 16% of cells were lysed, and could be distinguished from viable cells not only by live/dead staining but also by a characteristic “ghost”-like appearance in phase-contrast images (Fig. 1F, arrow). Interestingly, we found that the addition of 0.5M sucrose to the growth medium as an osmoprotectant reduced the number of lysed cells from 16% to 3% after 24 h exposure to meropenem (Fig. 1H, I). Osmoprotection was clearly not essential for spherical cell formation or viability, however, unless otherwise indicated, we chose to add 0.5M sucrose to the growth medium in subsequent experiments (Fig. 2-7) simply to minimize the small amount of cell lysis observed in standard laboratory broth.

Importantly, we also tested whether spherical cells can form under conditions relevant to infection and the *in vivo* environment. To this end PA14 cells were treated with meropenem (5x MIC) in a synthetic sputum medium designed to mimic the cystic fibrosis lung (15), as well as in fetal bovine serum. Note, sucrose was not added to these media. In both synthetic sputum and fetal bovine serum we observed a rapid transition of the cellular population from rods to spherical cells following treatment with meropenem, similar to that seen in standard growth media (Fig. S1). Therefore, *P. aeruginosa* spherical cells form in response to meropenem exposure under physiologically relevant conditions.

To confirm the spherical shape of meropenem-treated cells we used 3D-structured illumination microscopy (3D-SIM), a super resolution fluorescence technique that enables genuine 3D images of bacterial cells and reveals morphological details not visible with conventional microscopy through increases in both lateral and axial resolution (18) (Fig. 2). We also used 3D-SIM to examine the transition from rod to sphere, and found that it begins with the emergence of a small

membrane protrusion on the cell surface (Fig. 2B). This gradually bulges out to form a larger sphere, which becomes completely enclosed in its own membrane. The original rod then lyses, leaving a mature, spherical cell (Fig. 2B, C).

### *P. aeruginosa* spherical cells have a defective cell wall and disrupted outer membrane

The bacterial cell wall is a key structural feature of the cell that determines its shape and serves as an important osmotic barrier to the external environment. The loss of cell shape observed after meropenem treatment of *P. aeruginosa*, together with the slight osmosensitivity of the resulting spherical cells (see above), strongly suggests that these cells lack a functional cell wall. In addition, we found that spherical cells rapidly burst when placed directly between a microscope slide and a coverslip, indicating a mechanical fragility consistent with loss of integrity in the cell envelope.

To further examine the cell envelope structure of the spherical cell morphotype, we performed transmission electron microscopy (TEM) on thin sections of PA14 cells after 24 h exposure to meropenem. We also examined untreated cells as a control, and as expected these cells exhibited a regular double membrane cell envelope structure characteristic of Gram negative bacteria (Fig. 3A, B). In spherical cells, however, the outer membrane was clearly disrupted in all cells examined (Fig. 3C, D; 82 cells were analysed in total). While fragments of outer membrane remained associated with the cell (Fig. 3C), there were extensive regions in which the inner membrane appeared to be exposed on the cell surface. Interestingly, membrane vesicles were often observed to form apparently from outer membrane material that had detached from the cell envelope (Fig. 3C, D). Taken together, these results indicate that *P. aeruginosa* cells can convert

to an alternative form deficient in an intact cell wall and outer membrane when challenged with a cell wall-targeting antibiotic.

#### *The transition to spherical cells is readily reversible*

To test whether *P. aeruginosa* PA14 spherical cells induced by meropenem treatment can revert to normal rod shaped cells in the absence of antibiotic selection, we resuspended spherical cells formed after 24 h exposure to meropenem in fresh media lacking the drug. Cells were then visualized at regular intervals by phase-contrast microscopy and 3D-SIM. Under these conditions, we observed a rapid population-wide transition of the cellular population from spherical cells back to normal bacillary cells (Fig. 4). The first visible sign of this reversion was a change from a spherical to an ellipsoid morphology, which could be seen in some cells after just 30 min in the absence of drug. This was followed by a gradual elongation in cell length and reduction in width to produce a normal cylindrical cell. High resolution 3D-SIM images showed that the cell surface was highly irregular, sometimes even branched, during this reversion process, but ultimately became smooth and uniform as the normal cell wall was restored (Fig. 4E). After 6 h in the absence of antibiotic, the vast majority of the cellular population (>90%) had completed the transition to rods (Fig. 4F). These cells were able to grow and divide normally, as evidenced by a rapid increase in the density of cells in culture following reversion to the rod shape (Fig. 4C-D). This indicates that the transition to spherical cells following exposure to meropenem is readily reversible.

#### *Spherical cell formation is a conserved mechanism of meropenem tolerance*

Importantly, we observed that the ability to transition into and out of the spherical cell state occurred independently of strain background. An identical response to meropenem treatment was

seen for a wide variety of *P. aeruginosa* strains, including well known lab strains (PA14, PAO1, PA103, PAK, ATCC27853) and recent clinical isolates (data not shown). This observation, along with the sheer speed, efficiency and reversibility of the rod to spherical cell transition, indicates that formation of spherical cells in *P. aeruginosa* does not depend on the acquisition of chromosomal mutations. Rather, our results suggest that spherical cell formation is an intrinsic protective response. By undergoing rapid *en masse* phenotypic transitions between bacillary and spherical cell morphotypes, the vast majority of the *P. aeruginosa* population are able to survive exposure to meropenem and are poised to transition to the bacillary form when antibiotic levels are reduced.

*Penicillins and carbapenems induce spherical cell-mediated antibiotic tolerance*

Having determined that *P. aeruginosa* PA14 cells quickly convert to a spherical cell morphotype when treated with meropenem, we were interested to determine whether other cell wall-targeting antibiotics can elicit a similar response. Interestingly, *P. aeruginosa* has previously been shown to induce “spheroplasts” in response to carbenicillin (19), a penicillin derivative, and we reasoned that these spherical cells could facilitate tolerance to the drug. We found that following treatment of PA14 with carbenicillin (5x MIC), a large proportion of cells indeed converted to spherical cells and did so via the same morphological pathway that we observed in response to meropenem exposure (Fig. 5). In contrast to meropenem, however, some cells became filamentous rather than converting to the spherical cell state (Fig. 5). While filamentation is a common phenotype associated with  $\beta$ -lactam treatment in rod-shaped bacteria (3, 20), we found that the *P. aeruginosa* filamentous cells arising under these conditions tended to lyse. Live/dead staining with Syto9 and propidium iodide showed that the filamentous cells stained with propidium iodide

indicating that they were non-viable (Fig. 5C) whereas the spherical cell morphotypes stained only with Syto9 and were therefore viable. As was observed after removal of meropenem, the population of carbenicillin-induced spherical cells rapidly reverted to normal bacillary cells when resuspended in fresh media lacking the antibiotic (data not shown).

We also examined the effect of imipenem (5x MIC) on *P. aeruginosa* PA14 cells. Like meropenem, imipenem is a carbapenem antibiotic and we found that this also induced a rapid and reversible transition of the entire cellular population to spherical cells (Fig. S2). Taken together, these results demonstrate that spherical cell-mediated antibiotic tolerance in *P. aeruginosa* can occur in response to  $\beta$ -lactams from at least two classes.

*Meropenem-induced spherical cells are efficiently killed by antimicrobial peptides*

Having established that *P. aeruginosa* cells convert very rapidly and efficiently to cell wall deficient spherical cells when treated with  $\beta$ -lactam antibiotics, we hypothesized that the combination of a  $\beta$ -lactam that induces spherical cell formation with a drug that kills spherical cells could be feasible as a new and effective treatment approach for *P. aeruginosa* infections. One class of compounds that we reasoned might exhibit strong spherical cell killing activity were antimicrobial peptides (AMPs). These compounds function by direct interaction with membrane lipids and are thought to induce cell death through the formation of pores in the cytoplasmic membrane (21). Our TEM images show that there are vast stretches of cytoplasmic membrane exposed on the surface of spherical cells (Fig. 3) which should therefore be much more accessible to AMPs. Importantly, AMPs tend to have only weak antimicrobial activities against normal bacillary cells of *P. aeruginosa* under physiological conditions (22).



262

263 To test our hypothesis, cultures of *P. aeruginosa* PA14 were treated with a combination of  
264 meropenem to induce spherical cell formation (at a fixed concentration of 5 µg/mL) and one of  
265 the AMPs LL-37 or nisin (at various concentrations between 0 and 128 µg/mL). After 24 h in the  
266 presence of the drug combinations, viable cell counts were determined by serial dilution and  
267 plating. While meropenem alone produced viable spherical cells, the addition of LL-37 or nisin  
268 markedly reduced viability (Fig. 6A). In fact, at the highest AMP concentration tested (128  
269 µg/mL), viable cell counts were more than 3-4 log lower than those of the meropenem only  
270 control. IC<sub>50</sub> values were 16 µg/mL for nisin and 32 µg/mL for LL-37 in combination with  
271 meropenem. The strong bactericidal activity of the meropenem/AMP combinations was further  
272 highlighted by a distinct absence of intact cells under the microscope, replaced with what  
273 appeared to be cellular debris (Fig. 6B-D). Importantly, under our assay conditions the AMPs  
274 alone (LL-37 or nisin) showed no detectable antibacterial ability (Fig. 6E-H) even at the highest  
275 concentration tested (128 µg/mL). This is consistent with the high MIC values recently reported  
276 for LL-37 against PA14 cells under similar conditions (23) (112 – 225 µg/mL). These  
277 observations suggest, as predicted, that AMPs are more effective against spherical cells than  
278 normal bacillary cells, which we further confirmed by demonstrating that the AMPs can  
279 efficiently kill pre-formed *P. aeruginosa* spherical cells (Fig. S3).

280

281 Finally, time-kill assays were performed with PA14 to examine the rate of meropenem/AMP-  
282 induced cell death (Fig. 7A). Both LL-37 and nisin triggered a rapid decline in viability when  
283 administered in combination with meropenem. A 100-fold reduction of viable cell counts relative  
284 to the meropenem only control was observed within just 1 h for LL-37 and 8 h for nisin and by

24 h viability was reduced by 4-5 log for both AMP/meropenem combinations. Interestingly, the rapid killing by LL-37 suggests that only a partial transition of the cell to the spherical cell state is required for the AMP to mediate killing. We confirmed this for LL-37 using time-lapse microscopy, which showed that the peptide causes the cell to burst at the site of spherical cell formation (Fig. 7B).

## Discussion

Currently there is a desperate need for innovative approaches to antimicrobial therapy. This stems from a relentless rise in the emergence of antibiotic resistant bacteria, a lack of new antibiotic classes in the pharmaceutical pipeline, and greatly reduced investment within the pharmaceutical sector (24-26). Our data show that it is possible to effectively kill bacteria by turning their own biological responses against them, namely using drug combinations that induce the cell to transition to an alternative form then exploit the inherent weaknesses of that form. Drug combinations are commonly used in medicine to enhance the effectiveness of existing antibiotics (24), and represent a promising avenue for the development of new treatments (27-29) with reduced rates of resistance (30). In this study we have shown that combinations of meropenem with AMPs LL-37 or nisin are potently bactericidal against *P. aeruginosa* at concentrations where each drug alone has negligible bactericidal activity. Our findings provide a platform to identify novel antibacterial drug combinations that induce and target spherical cells in a directed and cost effective manner.

Significantly, our observations suggest that the ability to switch between bacillary and spherical cell morphotypes is a response to stress invoked by exposure to  $\beta$ -lactam antibiotics. Transition

of *P. aeruginosa* to the spherical state occurred rapidly in response to  $\beta$ -lactams from the carbapenem and penicillin classes, and was found to be independent of genetic background. These results suggest that spherical cell formation may be an intrinsic developmental response of *P. aeruginosa* that is induced by antibiotic treatment. Whilst the production of spherical cells by carbapenems and penicillins has been reported previously (7, 8, 19), our observations show for the first time that spherical cell formation is reversible and occurs readily under physiological conditions, indicating that this response may serve as a genuine mechanism of drug tolerance.

We propose that spherical cell-mediated  $\beta$ -lactam tolerance may underlie many of the pharmacodynamic challenges associated with  $\beta$ -lactam treatment of *P. aeruginosa* infections (12-14), at least in the case of carbapenems and penicillins. *P. aeruginosa* infections are notoriously difficult to treat and are often chronic or recurrent in nature, particularly in immunocompromised patients (31). It is tempting to speculate that the transition of *P. aeruginosa* to a viable alternative spherical cell morphotype during exposure to  $\beta$ -lactams could lead to prolonged or recurrent infections by allowing the bacterium to survive *in vivo* over the course of antibiotic treatment and then to revert to the bacillary form when antibiotic therapy is ceased.

Significantly, spherical cell formation may also play an important role in the emergence of  $\beta$ -lactam resistance. Spontaneous  $\beta$ -lactam resistant mutants of *P. aeruginosa* are known to arise quite readily *in vitro* during antibiotic treatment (12, 14). Here we have shown that *P. aeruginosa* can undergo *en masse* transition to cell wall defective spherical cells under these conditions. While in the spherical form the population would be well poised to acquire  $\beta$ -lactam resistance, either by mutation or lateral gene transfer (1), which would enable reversion to the bacillary form

and rapid cell proliferation. Consistent with this idea, early studies on carbenicillin-induced spheroplasts of *P. aeruginosa* showed that cells spontaneously reverted to rods after extended exposure to the drug (5-8 days), and that the MIC of carbenicillin increased as much as 150-fold following reversion (19, 32). Critically, we now show that a carbapenem in combination with antimicrobial peptides induces rapid killing of *P. aeruginosa* cells. This type of approach would severely limit the potential for acquiring resistance during  $\beta$ -lactam therapy.

A classic problem in population and evolutionary biology is to understand how a population copes with environmental changes that challenge survival. Common strategies that enable survival of antibiotic exposure by bacterial populations include selection of a sub-population that has a fitness advantage that can arise either through mutation, stochastic phenotypic heterogeneity or regulated responses (33). Our observations suggest that tolerance to  $\beta$ -lactam exposure by *P. aeruginosa* can occur through an adaptive response that involves *en masse* phenotypic transitions between bacillary cells and spherical cells with defective cell walls. Therefore, population-wide morphotype transitions add to the repertoire of strategies that can be employed by bacteria to survive exposure to  $\beta$ -lactam antibiotics.

**Acknowledgments** C.B.W. was supported by an Australian National Health and Medical Research Council Senior Research Fellowship (571905). L.G.M. was supported by an institute Postdoctoral Fellowship. L.T. was supported by a UTS Chancellor's Postdoctoral Fellowship.

354

355 **References**

- 356 1. **Poole K.** 2011. *Pseudomonas aeruginosa*: resistance to the max. Front. Microbiol. **2**:65.
- 357 2. **Hamad B.** 2010. The antibiotics market. Nat. Rev. Drug Discov. **9**:675-676.
- 358 3. **Kong KF, Schneper L, Mathee K.** 2009. Beta-lactam antibiotics: from antibiosis to  
359 resistance and bacteriology. APMIS **118**:1-36.
- 360 4. **Bush K.** 2012. Antimicrobial agents targeting bacterial cell walls and cell membranes.  
361 Rev. Sci. Tech. **31**:43-56.
- 362 5. **Spratt BG, Cromie KD.** 1988. Penicillin-binding proteins of Gram-negative bacteria.  
363 Rev. Infect. Dis. **10**:699-711.
- 364 6. **Tomasz A.** 1986. Penicillin-binding proteins and the antibacterial effectiveness of beta-  
365 lactam antibiotics. Rev. Infect. Dis. **8**, Suppl. **3**:S260-278.
- 366 7. **Trautmann M, Heinemann M, Zick R, Moricke A, Seidelmann M, Berger D.** 1998.  
367 Antibacterial activity of meropenem against *Pseudomonas aeruginosa*, including  
368 antibiotic-induced morphological changes and endotoxin-liberating effects. Eur. J. Clin.  
369 Microbiol. Infect. Dis. **17**:754-760.
- 370 8. **Horii T, Kobayashi M, Sato K, Ichiyama S, Ohta M.** 1998. An in-vitro study of  
371 carbapenem-induced morphological changes and endotoxin release in clinical isolates of  
372 Gram-negative bacilli. J. Antimicrob. Chemother. **41**:435-442.
- 373 9. **Nishino T, Nakazawa S.** 1976. Bacteriological study on effects of beta-lactam group  
374 antibiotics in high concentrations. Antimicrob. Agents Chemother. **9**:1033-1042.
- 375 10. **Chadwick P.** 1969. Effect of carbenicillin on *Pseudomonas aeruginosa*. Can. Med.  
376 Assoc. J. **101**:74-80.

- 377 11. **Zar FA, Kany RJ, Jr.** 1985. In vitro studies of investigational beta-lactams as possible  
378 therapy for *Pseudomonas aeruginosa* endocarditis. Antimicrobial. Agents Chemother.  
379 **27**:1-3.
- 380 12. **Tam VH, Schilling AN, Melnick DA, Coyle EA.** 2005. Comparison of beta-lactams in  
381 counter-selecting resistance of *Pseudomonas aeruginosa*. Diagn. Microbiol. Infect. Dis.  
382 **52**:145-151.
- 383 13. **Burgess DS.** 2005. Use of pharmacokinetics and pharmacodynamics to optimize  
384 antimicrobial treatment of *Pseudomonas aeruginosa* infections. Clin. Infect. Dis. **40**,  
385 **Suppl 2**:S99-104.
- 386 14. **Tam VH, Schilling AN, Neshat S, Poole K, Melnick DA, Coyle EA.** 2005.  
387 Optimization of meropenem minimum concentration/MIC ratio to suppress in vitro  
388 resistance of *Pseudomonas aeruginosa*. Antimicrob. Agents Chemother. **49**:4920-4927.
- 389 15. **Palmer KL, Aye LM, Whiteley M.** 2007. Nutritional cues control *Pseudomonas*  
390 *aeruginosa* multicellular behavior in cystic fibrosis sputum. J. Bacteriol. **189**:8079-8087.
- 391 16. **Clinical and Laboratory Standards Institute.** 2003. Methods for dilution antimicrobial  
392 susceptibility tests for bacteria that grow aerobically. Sixth Edition: Approved Standard  
393 M7-A6, CLSI, Villanova, PA.
- 394 17. **Strauss MP, Liew AT, Turnbull L, Whitchurch CB, Monahan LG, Harry EJ.** 2012.  
395 3D-SIM super resolution microscopy reveals a bead-like arrangement for FtsZ and the  
396 division machinery: implications for triggering cytokinesis. PLoS Biol. **10**:e1001389.
- 397 18. **Gustafsson MG, Shao L, Carlton PM, Wang CJ, Golubovskaya IN, Cande WZ,**  
398 **Agard DA, Sedat JW.** 2008. Three-dimensional resolution doubling in wide-field  
399 fluorescence microscopy by structured illumination. Biophys. J. **94**:4957-4970.

- 400 19. **Watanakunakorn C, Hamburger M.** 1969. Induction of spheroplasts of *Pseudomonas*  
401 *aeruginosa* by carbenicillin. Appl. Microbiol. **17**:935-937.
- 402 20. **Justice SS, Hunstad DA, Cegelski L, Hultgren SJ.** 2008. Morphological plasticity as a  
403 bacterial survival strategy. Nat. Rev. Microbiol. **6**:162-168.
- 404 21. **Fjell CD, Hiss JA, Hancock RE, Schneider G.** 2012. Designing antimicrobial peptides:  
405 form follows function. Nat. Rev. Drug Discov. **11**:37-51.
- 406 22. **Hancock REW, Nijnik A, Philpott DJ.** 2012. Modulating immunity as a therapy for  
407 bacterial infections. Nat. Rev. Microbiol. **10**:243-254.
- 408 23. **Kapoor R, Wadman MW, Dohm MT, Czyzewski AM, Spormann AM, Barron AE.**  
409 2011. Antimicrobial peptoids are effective against *Pseudomonas aeruginosa* biofilms.  
410 Antimicrob. Agents Chemother. **55**:3054-3057.
- 411 24. **Wright GD.** 2012. Antibiotics: a new hope. Chem. Biol. **19**:3-10.
- 412 25. **Boucher HW, Talbot GH, Bradley JS, Edwards JE, Gilbert D, Rice LB, Scheld M,**  
413 **Spellberg B, Bartlett J.** 2009. Bad bugs, no drugs: no ESKAPE! An update from the  
414 Infectious Diseases Society of America. Clin. Infect. Dis. **48**:1-12.
- 415 26. **Piddock LJ.** 2012. The crisis of no new antibiotics: what is the way forward? Lancet  
416 Infect. Dis. **12**:249-253.
- 417 27. **Ejim L, Farha MA, Falconer SB, Wildenhain J, Coombes BK, Tyers M, Brown ED,**  
418 **Wright GD.** 2011. Combinations of antibiotics and nonantibiotic drugs enhance  
419 antimicrobial efficacy. Nat. Chem. Biol. **7**:348-350.
- 420 28. **Lehar J, Zimmermann GR, Krueger AS, Molnar RA, Ledell JT, Heilbut AM, Short**  
421 **GF, 3rd, Giusti LC, Nolan GP, Magid OA, Lee MS, Borisy AA, Stockwell BR, Keith**  
422 **CT.** 2007. Chemical combination effects predict connectivity in biological systems. Mol.  
423 Syst. Biol. **3**:80.

- 424 29. **Sharom JR, Bellows DS, Tyers M.** 2004. From large networks to small molecules. Curr.  
425 Opin. Chem. Biol. **8**:81-90.
- 426 30. **Walsh C.** 2000. Molecular mechanisms that confer antibacterial drug resistance. Nature  
427 **406**:775-781.
- 428 31. **Mesaros N, Nordmann P, Plesiat P, Roussel-Delvallez M, Van Eldere J, Glupczynski**  
429 **Y, Van Laethem Y, Jacobs F, Lebecque P, Malfroot A, Tulkens PM, Van Bambeke**  
430 **F.** 2007. *Pseudomonas aeruginosa*: resistance and therapeutic options at the turn of the  
431 new millennium. Clin. Microbiol. Infect. **13**:560-578.
- 432 32. **Watanakunakorn C, Phair JP, Hamburger M.** 1970. Increased resistance of  
433 *Pseudomonas aeruginosa* to carbenicillin after reversion from spheroplast to rod form.  
434 Infect. Immun. **1**:427-430.
- 435 33. **Ryall B, Eydallin G, Ferenci T.** 2012. Culture history and population heterogeneity as  
436 determinants of bacterial adaptation: the adaptomics of a single environmental transition.  
437 Microbiol. Mol. Biol. Rev. **76**:597-625.



## Figure Legends

### **Fig. 1. *P. aeruginosa* rapidly converts to spherical cells in response to a $\beta$ -lactam antibiotic.**

PA14 cells cultured in cation-adjusted Mueller Hinton broth (CAMHB) were treated with meropenem (5x MIC) and visualized by phase-contrast or fluorescence (live/dead) microscopy. (A-D) Phase-contrast images taken immediately prior to meropenem addition (A) and after 1 h (B), 4 h (C) and 24 h (D) in the presence of the drug. (E) Proportion of rods, spherical cells and transitioning cells in the population over time. 200 cells were scored from phase-contrast micrographs at each time point from 2 experiments. (F-I) Live/dead viability staining of meropenem-treated cells after 24 h. Cells were grown in CAMHB (F-G) or CAMHB supplemented with 0.5M sucrose (H-I). Samples were co-stained with SYTO9 (live, green) and propidium iodide (dead, red) and visualized by phase-contrast (F, H) and wide-field fluorescence microscopy (G, I). Arrow points to a lysed cell. Scale bars 5  $\mu$ m.

### **Fig. 2. Super resolution 3D-SIM microscopy showing the transition of *P. aeruginosa* to**

**meropenem-induced spherical cells.** Following treatment with meropenem, PA14 cells were stained with membrane dye FM1-43 and visualized by 3D-SIM. Images were acquired at 0 h (A), 2 h (B) and 24 h (C) after meropenem addition. Asterisk highlights a developing spherical cell that is fully surrounded by membrane. Arrow shows a cell at an earlier stage of the transition, containing a surface bulge that is not yet membrane-enclosed. Scale bars 1  $\mu$ m.

### **Fig. 3. Meropenem-induced spherical cells of *P. aeruginosa* have a compromised cell**

**envelope.** Transmission electron microscopy (TEM) was performed on thin sections of PA14 cells immediately prior to the addition of meropenem (A, B) and after 24 h in the presence of the

drug (C, D). Panels B and D are shown at high magnification to illustrate the cell envelope structure, revealing an intact outer membrane (black arrow) and inner membrane (white arrow) in the bacillary form (B) and a clearly disrupted outer membrane in the spherical cell (D). Arrow in C shows a vesicle that appears to have formed from detached outer membrane material. Scale bars 100 nm.

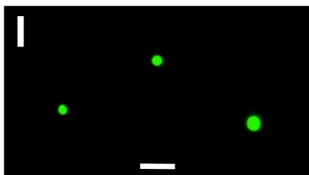
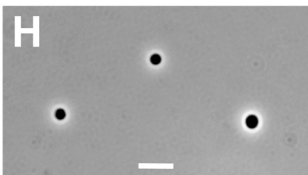
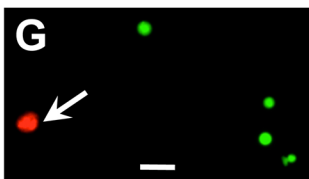
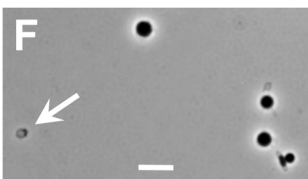
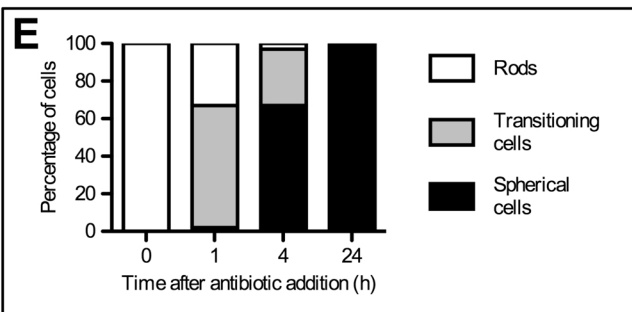
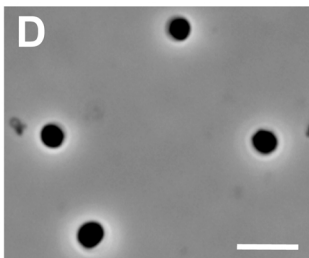
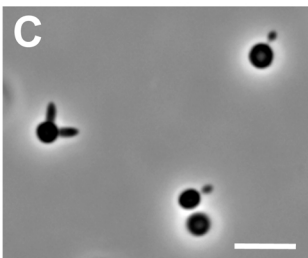
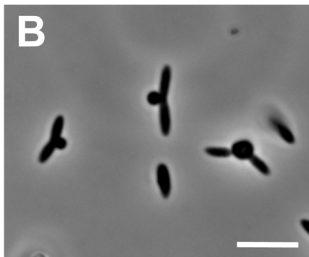
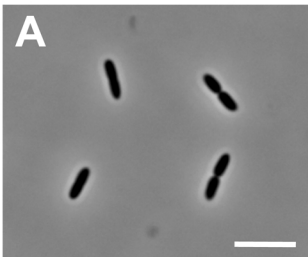
**Fig. 4. Spherical *P. aeruginosa* cells rapidly revert to normal rods in the absence of antibiotic.** Meropenem-induced spherical cells of PA14 were resuspended in antibiotic-free media and visualized by phase-contrast microscopy or 3D-SIM. (A-D) Phase-contrast images taken at 0 h (A), 2 h (B), 6 h (C) and 24 h (D) after removal of meropenem. (E) 3D-SIM images of FM1-43 stained cells captured at various stages in the transition from spherical cell (i) to normal rod (vi). (F) Proportion of spherical cells, rods and transitioning cells in the population over time. 200 cells were scored from phase-contrast micrographs at each time point from 2 experiments. Scale bars 5  $\mu\text{m}$  (A-D) or 1  $\mu\text{m}$  (E).

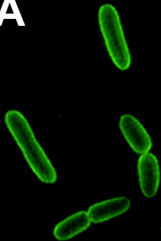
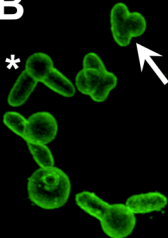
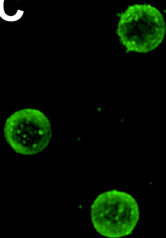
**Fig. 5. Spherical cells induced by carbenicillin.** (A-B) 3D-SIM images of PA14 cells stained with membrane dye FM1-43 after 2 h (A) and 24 h (B) in the presence of carbenicillin. (C) Live/dead viability staining of carbenicillin-treated cells after 24 h, showing viable spherical cells and a dead filamentous cell. Cells were co-stained with SYTO9 (live, green) and propidium iodide (dead, red) and visualized by wide-field fluorescence microscopy. (D) Proportion of rods, spherical cells, transitioning cells and filaments in the population over time. 200 cells were scored from phase-contrast micrographs at each time point. Scale bars 1  $\mu\text{m}$  (A-B) or 5  $\mu\text{m}$  (C).

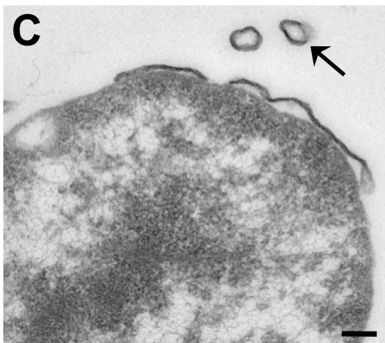
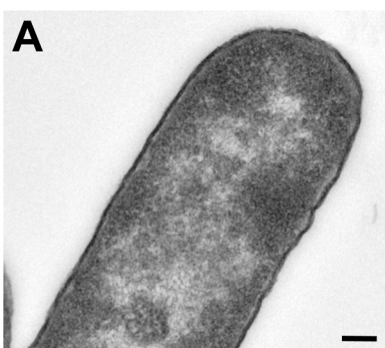
**Fig. 6. AMPs selectively kill meropenem-induced spherical cells of *P. aeruginosa*.** (A) Viable cell counts after treatment of PA14 for 24 h with a combination of meropenem (5  $\mu\text{g/mL}$ ) and either LL-37 or nisin (0-128  $\mu\text{g/mL}$ ). (B-D) Representative phase-contrast images of cells treated under the same conditions as in A. (B) Meropenem only control (no peptide), showing intact spherical cells. (C) LL-37 (128  $\mu\text{g/mL}$ ) with meropenem. (D) Nisin (128  $\mu\text{g/mL}$ ) with meropenem. Cellular debris can be seen in place of intact cells for both AMP/meropenem combinations. (E) Viability counts for untreated cells and cells treated with LL-37 or nisin alone (128  $\mu\text{g/mL}$ ). (F-H) Corresponding phase-contrast images. (F) Untreated control, showing normal rod shaped cells. (G) LL-37. (H) Nisin. Neither AMP alone appears to have any effect on cellular morphology. Scale bar 5  $\mu\text{m}$ . For (A) and (E) one representative data set is shown from duplicate (A) or triplicate (E) experiments. Error bars correspond to the standard error of the mean for triplicate measurements.

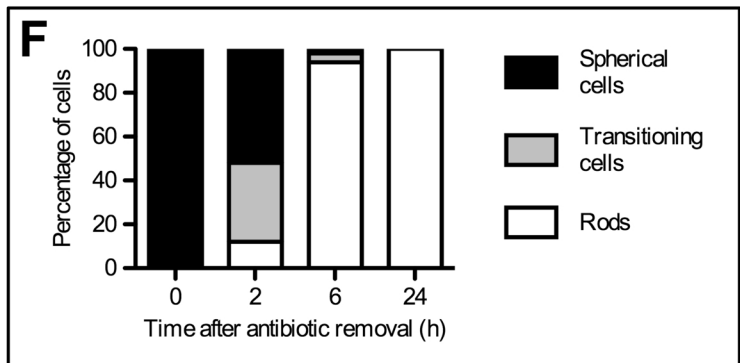
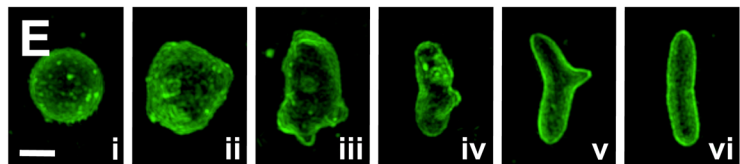
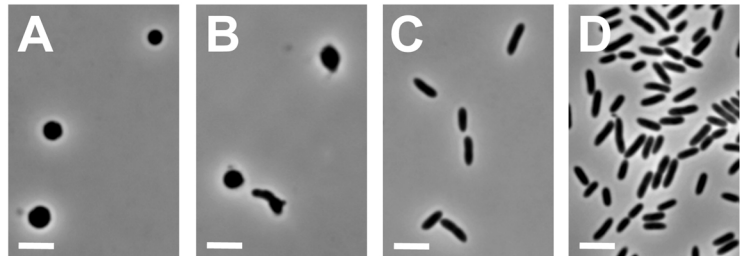
**Fig. 7. Meropenem and AMP combinations induce rapid cell death.** (A) Time-kill assay. Viable cell counts were measured at regular intervals after the addition of meropenem (5  $\mu\text{g/mL}$ ), both alone and in combination with LL-37 or nisin (128  $\mu\text{g/mL}$ ), to a culture of PA14 cells. One representative data set from duplicate experiments is shown. Error bars correspond to the standard error of the mean for triplicate measurements. (C) Time-lapse microscopy capturing the peptide-mediated death of a developing spherical cell. PA14 cells were treated with meropenem (5  $\mu\text{g/mL}$ ) for 1 h to induce a partial transition to the spherical state. LL-37 (128  $\mu\text{g/mL}$ ) was then added, and phase-contrast images were collected at 2 s intervals over a period of 30 min. In the example shown, panel i was acquired 13 min after the addition of the peptide, and each

508 subsequent image after an additional 2 s. A total of 13 individual cell death events were observed  
509 over four separate experiments. Scale bar 1  $\mu\text{m}$ .

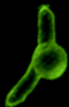
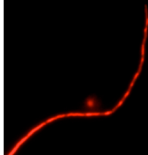


**A****B****C**







**A****B****C****D**